

# BioRID-II Dummy Model Development

--

## Stochastic Investigations

Sebastian Stahlschmidt\*, Bastian Keding\*, Katharina Witowski\*,  
Heiner Müllerschön\*, Uli Franz\*

\*DYNAmore GmbH, Stuttgart, Germany, <http://www.dynamore.de>

Contact: [sebastian.stahlschmidt@dynamore.de](mailto:sebastian.stahlschmidt@dynamore.de)

### Abstract:

Whiplash injuries may occur in low speed rear crashes. Many consumer and insurance organizations use the BioRID-II dummy as test device, to assess the risk of whiplash injuries in car accidents. An LS-DYNA model of the BioRID-II dummy has been developed by DYNA*more* GmbH in cooperation with the German Automotive Industry.

This paper describes the current validation state and shows the latest modifications of the BioRID-II model. The emphasis is to discuss observations made during validation. Additionally, the paper describes a robustness study of a validation load case. Robustness studies are performed during validation in order to investigate dependencies and stability of the measured quantities. For this a Monte Carlo Analysis using LS-OPT [7] is applied and statistical quantities are evaluated and displayed.

### Keywords:

BioRID, dummy, whiplash, robustness study, validation, LS-OPT, Monte Carlo Analysis

## 1 Introduction

Whiplash [1] is an injury that may occur in low speed rear impact scenarios in passenger cars. Even in the eighties studies to investigate the whiplash risks were performed. Initially, the HIII 50percentile dummy with its stiff spine and its simple neck was used. But even adaptations to the neck couldn't compensate the limited possibilities to capture injury criteria for whiplash scenarios.

In the 90's the Chalmers University of Technology of Sweden developed the BioRID (Biofidelic Rear Impact Dummy) in corporation with Saab and Volvo. The dummy is equipped with a detailed flexible spine and neck. Head, pelvis and extremities are modified parts also used in the HIII dummy. An enhanced version of the BioRID, the BioRID-II is currently used in insurance and consumer tests to assess seat designs. All tests use the dummy in a simple sled test with seat and a simplified restraint system. Due to the dominantly elastic deformations in the seat during the whiplash tests, it is difficult to detect the different load paths between the dummy and the seat. Consequently, simulation can reduce tests which are required to understand the load mechanisms, significantly. A working group of the FAT (German Association for Automotive Research) was launched in 2004 to guide development a finite element model of the BioRID-II. Participating companies are Audi, BMW, Mercedes, Porsche, Keiper Recaro, Hammerstein, Johnson Controls, Volkswagen and Karmann. During the project the FAT is defining tests, requirements and approves the models. Like in former dummy modeling projects DYNAmore is responsible for developing the LS-DYNA model. The model is commercially available for companies not participating in the project.

Previous releases of the model and the project itself have already been presented in papers [3] and [4]. The paper describes the work and observations during the current validation of the model. The emphasis of the presented graphs is to showcase effects rather than presenting the performance in a specific test. The correlation in the entire set of component and sled tests is presented in [2]. After the description of new features the paper presents a stochastic investigation carried out to understand the dummy behavior and stability.

## 2 Model Outline and Latest Modifications

The current commercial release of the BioRID-II model is version 1.5. It is available since May 2006. The model is based on CAD data from the dummy manufacturer Denton CAE for the BioRID-II specific parts and scanned data for parts also used in Hybrid III dummies. The masses are adapted according to a detailed measurement of each part.

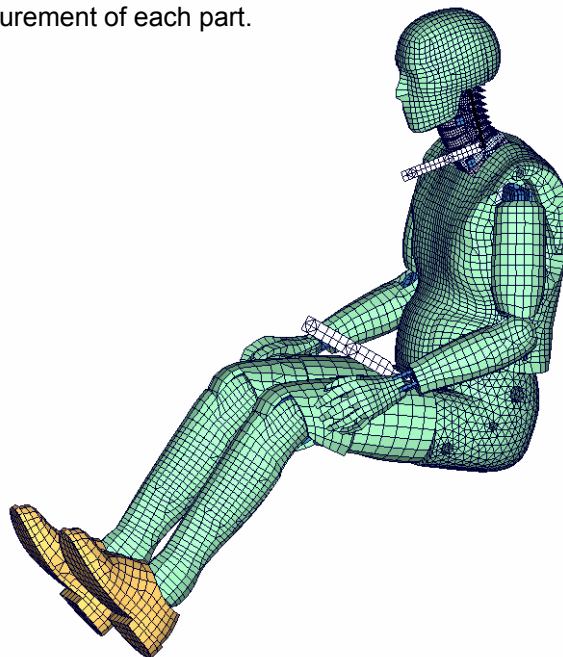


Figure 1: FAT LS-DYNA BioRID-II dummy model release 1.5.

Release 1.5 consists of approximately 146,000 nodes, 89,000 hexahedron elements, 22,000 tetrahedron elements, 71,000 shell elements, 4,000 beam elements and a couple of discrete elements. The model uses 45 different material definitions in 380 parts.

Figure 1 depicts the model release 1.5.

The model is delivered with a pre-stressed neck. Therefore, the bumpers in the neck use the feature `*INITIAL_FOAM_REFERENCE_GEOMETRY`. The pre-tensioned cable/springs use offsets in the force displacement relation. The torsional beams are modeled by `*CONSTRAINED_JOINT_STIFFNESS_GENERALIZED` with local coordinate systems attached to the washers. These features allow that a once positioned dummy can be used as an ASCII input file without losing any pre-stress in the model in the neck and the spine. Hence, the common procedure to use the `*INCLUDE` command to generate a final input is applicable. The determination of pre-stress is presented in [3].

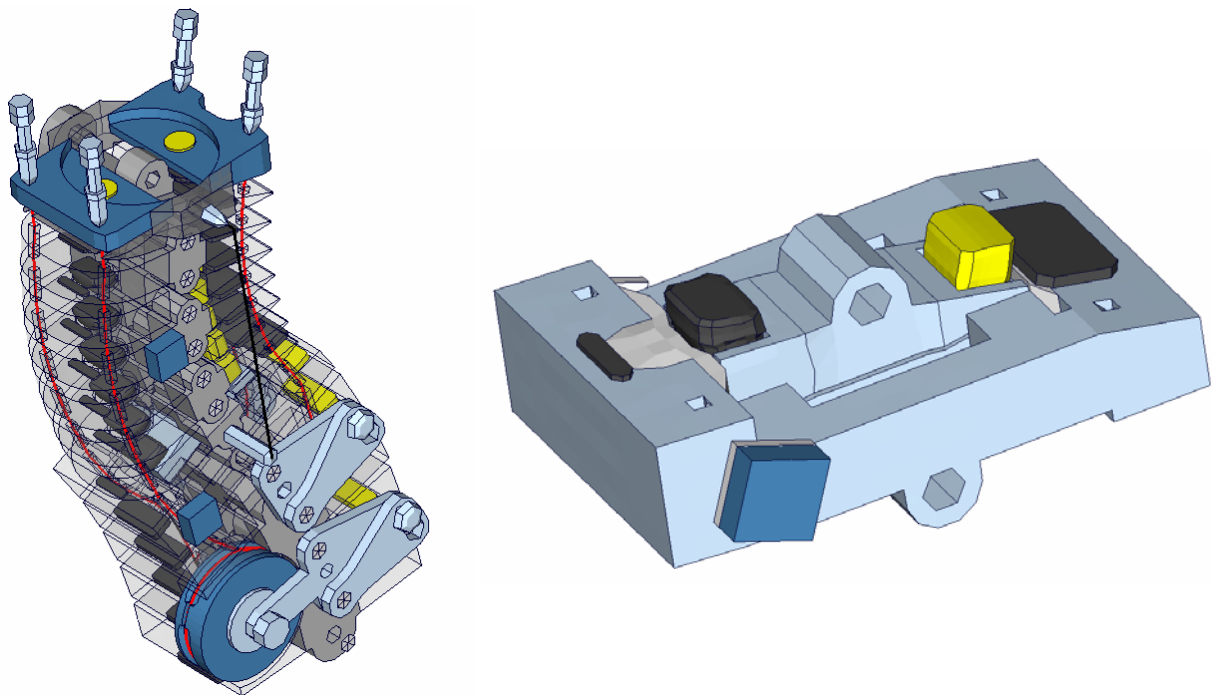


Figure 2: Selected parts of dummy model. Left: Neck model, with steel cable in red. Right: new modeled T1 load cell.

Majority of the latest validation work is on the kinematics of the neck. Thereby, T1 load cell (see Figure 2 right hand side) is refined and modeled more accurate. The rubber bumpers are now modeled in a pit which hinders the lateral strain. Also the silicon charge of the gaps in the load cell is modeled at selected points.

Also the rotational relationship between the vertebrae will be included in next release. Due to contact of the neck vertebrae C2 – C7 the relative rotation between these vertebrae is limited for rotations to the front. The rotations to the back are only limited by the bumpers.

Furthermore, the material model of the rubber bumpers will change. The latest official release uses the `*MAT_MOONEY-RIVLIN_RUBBER` for these parts. The next release will use the `*MAT_SIMPLIFIED_RUBBER` for the bumpers to enhance the kinematics and the strain rate dependency of the rubber bumpers. Therefore, the keyword `*INITIAL_FOAM_REFERENCE_GEOMETRY` had to be added in LS-DYNA for this material model. That is the reason why the next release of the BioRID-II runs with LS-DYNA 971. This step in the development of the BioRID-II was necessary to model the sensitive kinematics of the neck with higher accuracy. With

\*MAT\_SIMPLIFIED\_RUBBER we are able to capture much more details for the neck kinematics and the oscillation problem of the upcoming releases is decreased significantly.

The BioRID-II model can be handled like other FE dummy models. The extremities can be positioned in use of a normal pre-processor. To pre-stress the BioRID-II model there are no other files necessary. The pre-stress is applied full automatically by LS-DYNA. This is also valid if the initial position is determined by a pre-simulation and new nodal coordinates are used.

### 3 Material tests, component tests and fully assembled dummy test

A significant effort was made to generate a database on the static and dynamic material behavior, and the dummy behavior in component and fully assembled tests. A more detailed description of the material tests is presented in [4].

#### 3.1 Material tests

For each important material in the BioRID-II different tests with static and dynamic tension and compression loads were performed. The considered strain rates vary from 0.001 to 500 1/s. Figure 3 shows some selected material samples which are used for the material tests. The tests were chosen to obtain material data that could be used with very small adaptations for material \*MAT\_FU\_CHANG\_FOAM and \*MAT\_SIMPLIFIED\_RUBBER.

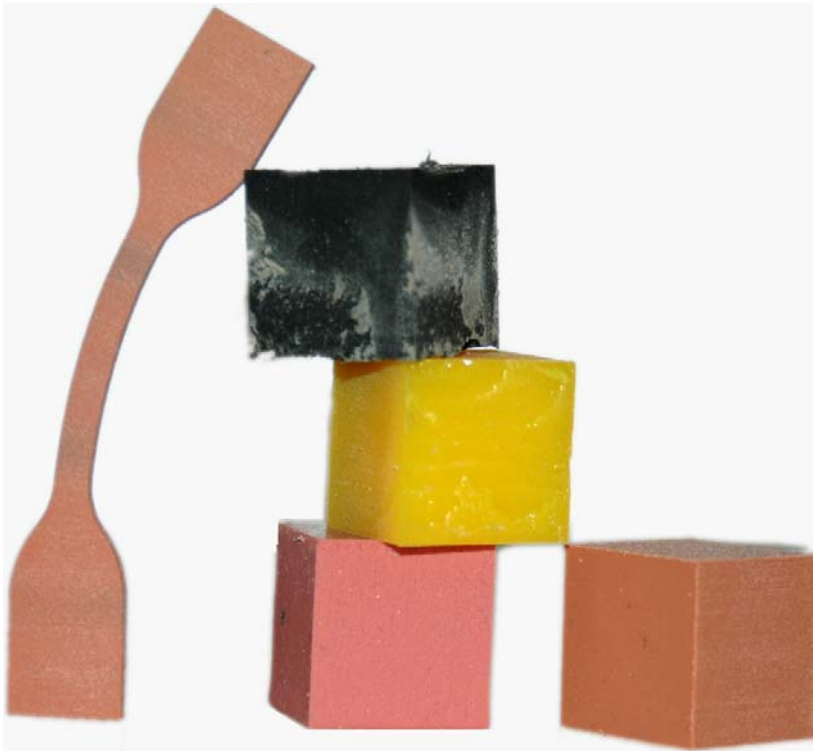


Figure 3: Material blocks for compression tests and a tension test sample.

### 3.2 Component tests

To get more understanding on the kinematics of the spine component tests were performed. Most of these tests investigate behavior of the fully and partially assembled spine. In

Figure 4 and Figure 5 different component tests are depicted. The tests were usually taken with different pulses.

Figure 4: Left: BioRID-II component test with supported spine. Right: Component test of assembled thorax.

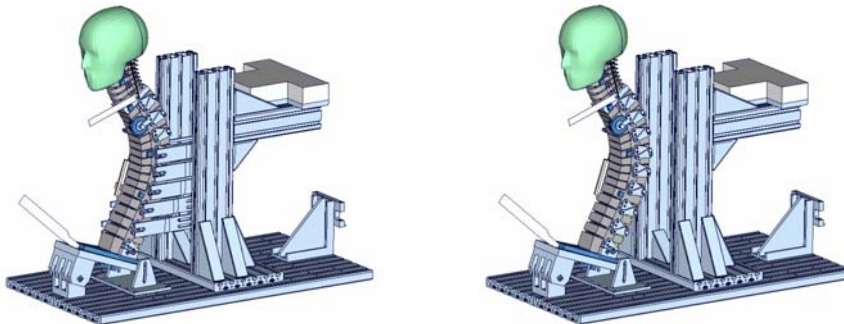


Figure 5: Left: BioRID-II component test with partially supported spine. Right: Component test with not supported spine.

More details are presented in [4]. The performance of the current release in the extensive number of tests is presented in the user manual of the dummy model [2].

Exemplarily, a test with the spine coupled to the sled from the spine adapter plate up to the T1 vertebra is showcased in the following. Only the neck with the assembled head can move. The test setup is depicted in

Figure 4 on the left hand side. The neck is equipped with damper and the pre-stressed steel cable. Figure 6 depicts the model at different stages during the test.

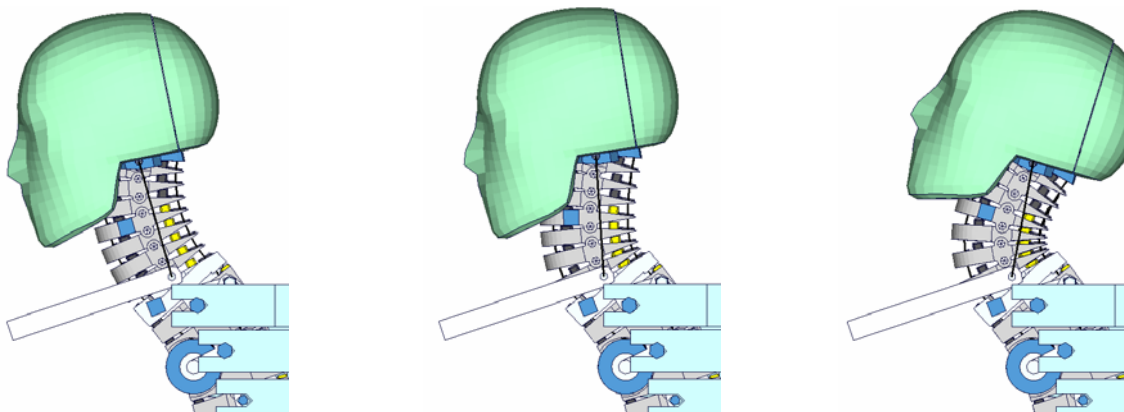


Figure 6: Spine, neck, and head in component test at 0, 45, and 125 ms.

It can be observed that in the first 45 ms the head is only rotating slightly. The dominant movement is a translation backwards and the deformation is a shear deformation between the head and the T1 vertebra. The motion in the first few milliseconds is very dependent on the pre-stress, the lateral strain of the rubber bumpers and the right rotation relationship between the vertebrae. Figure 7 to Figure 11 show the results of this load case.

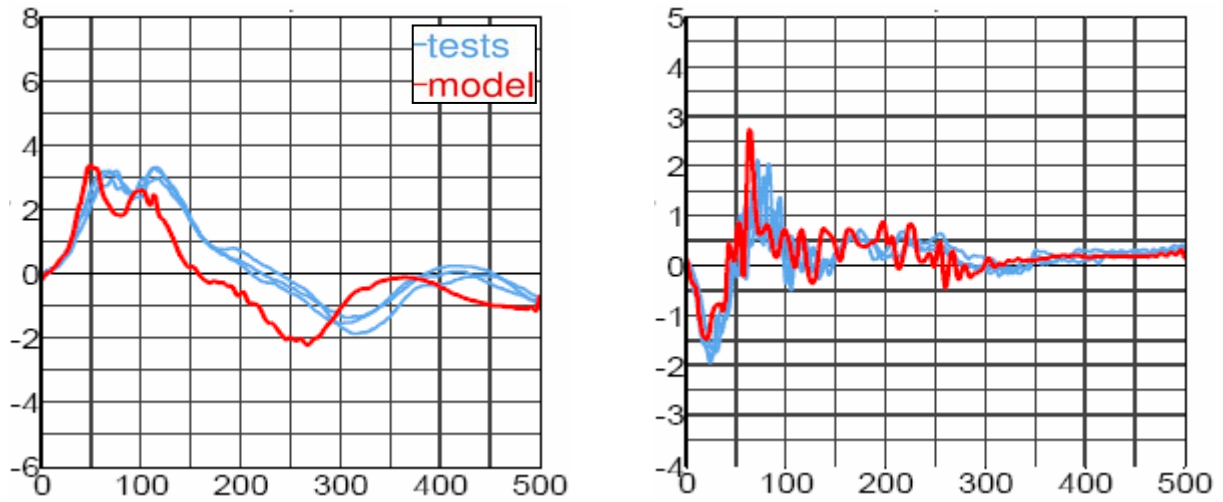


Figure 7: Head acceleration [g] vs. time [ms]. Left: x-acceleration. Right: z-acceleration.

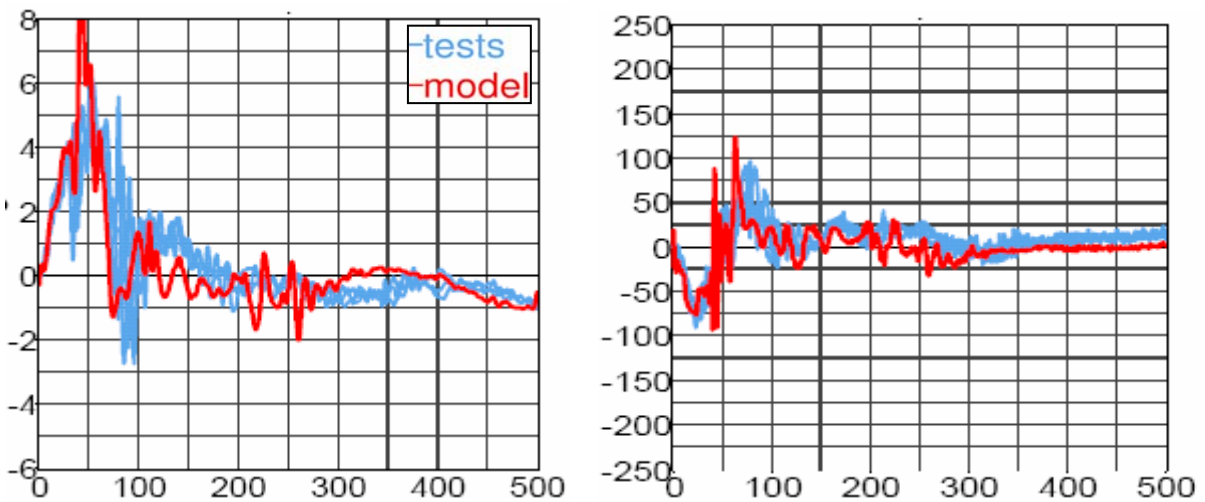


Figure 8: Neck acceleration [g] vs. time [ms] at C4. Left: x-acceleration. Right: z-acceleration.

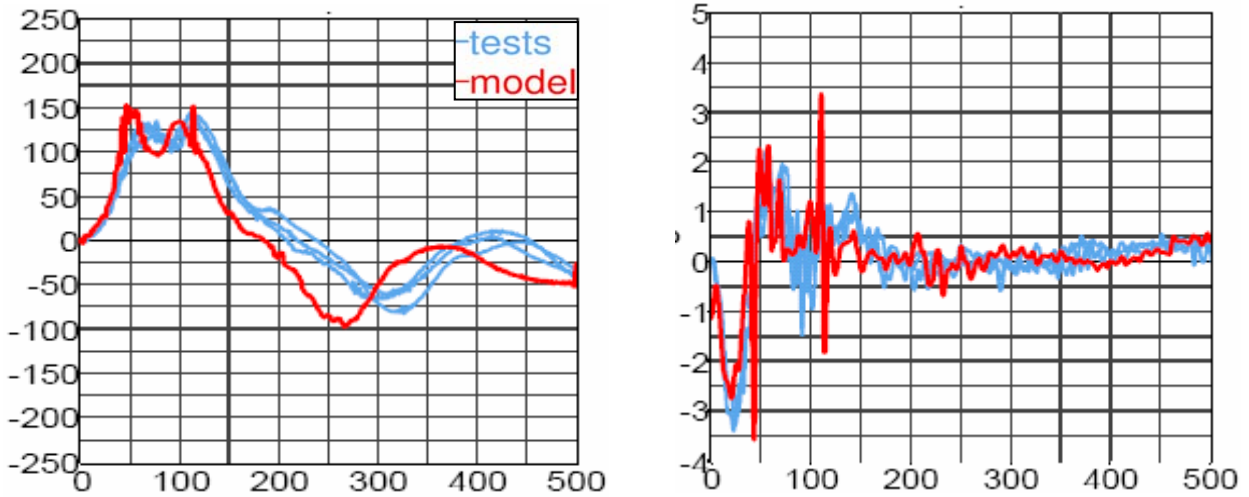


Figure 9: Upper neck force [N] vs. time [ms]. Left: Force in x direction. Right: Force in z direction.

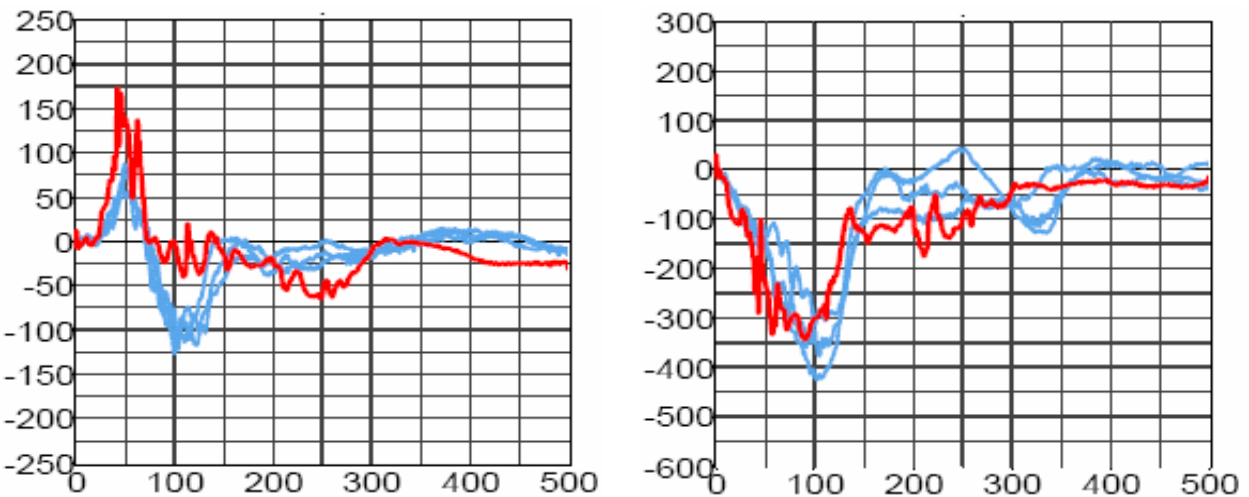


Figure 10: Lower neck force [N] vs. time [ms]. Left: Force in x. Right: Force in z direction.

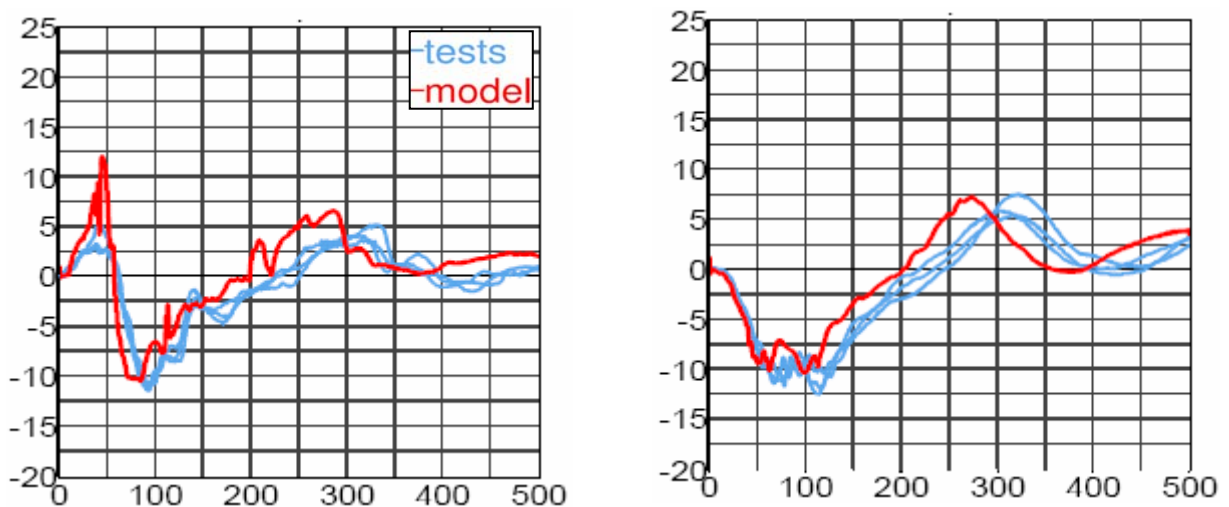


Figure 11: Left: Upper neck moment [Nm] along y vs. time [ms]. Right: Lower neck moment [Nm] along y vs. time [ms].

The double peak in the head x-acceleration (Figure 7 left) and in the upper neck x-force (Figure 9 left) is determined by the frictional dependency between the vertebrae. Also the peak in Figure 11 on the left hand side for the upper neck y-moment has a high dependency of these friction values.

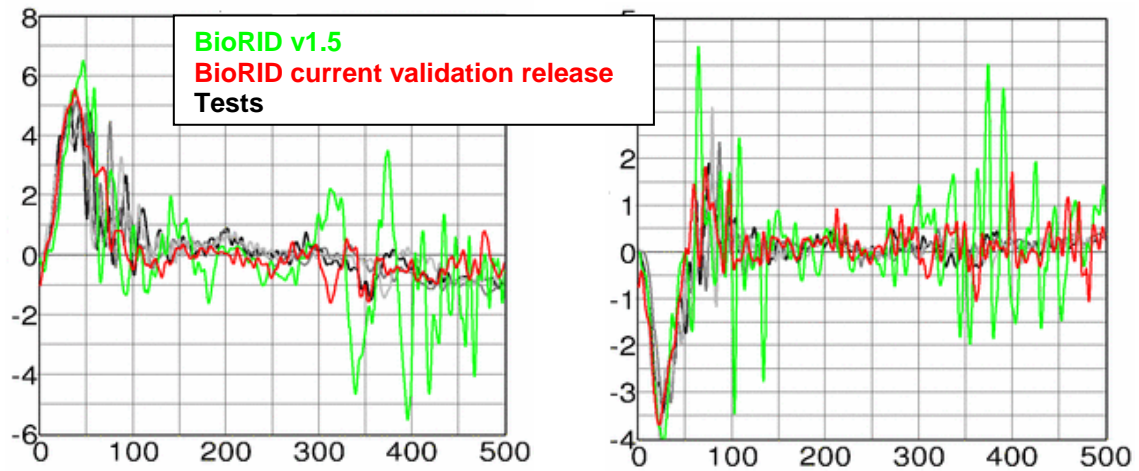


Figure 12: Neck acceleration [g] vs. time [ms] at T1. Left: x-acceleration. Right: z-acceleration.

The oscillations of T1 are decreased very much in the upcoming release, as depicted in Figure 12. This was achieved by using the new material model for the rubber bumpers. This is a comparison between BioRID v1.5 (green line) and the current validation release (red line). The black lines are the test results. The shown test is depicted in Figure 5 on the left hand side. The spine is fixed to the sled from the pelvis adapter plate up to T8. The thoracic and neck vertebrae can move freely.

### 3.3 Full assembled dummy tests

Since the current seat systems are very complex a simplified seat system was used to validate the dummy model. The seat used for the tests, is a modified version of a seat that originally was built at Chalmers University to develop the BioRID dummy [5]. This simplified seat is depicted in Figure 13.

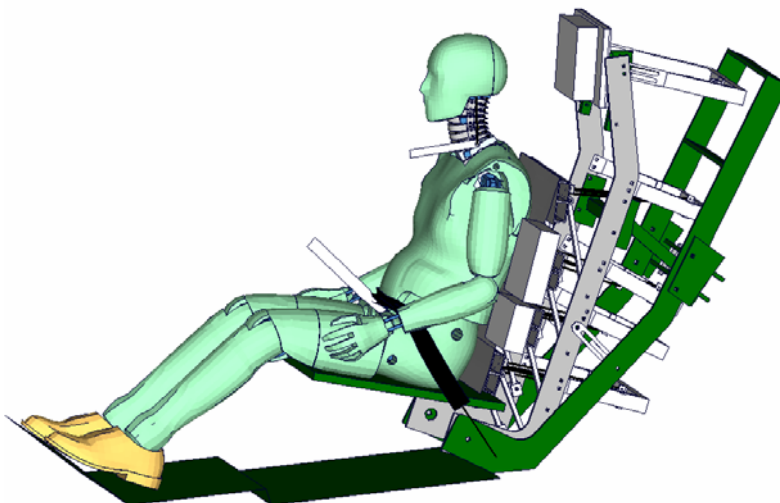


Figure 13: Full assembled dummy test.

In the tests the seat is accelerated with three different pulses. The pulses are used from the EuroNCAP proposal for whiplash tests. In the following the results of a 5g trapezoidal pulse are shown. Detailed information on the seat are presented in [4]. The used BioRID-II release is the same as in the component test presented above. The results of the simulation are the red lines and the test results are the blue lines.

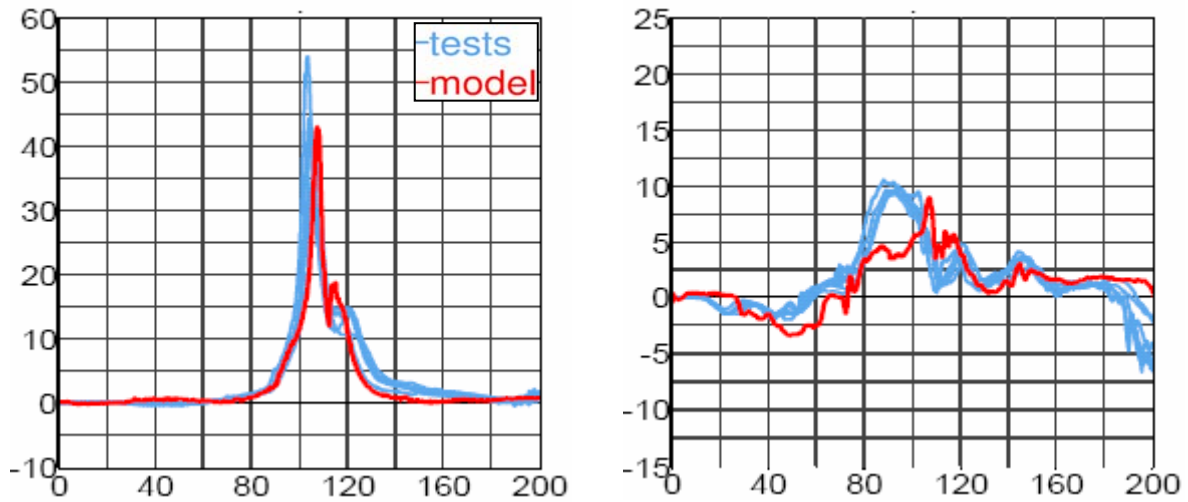


Figure 14: Head acceleration [g] vs. time [ms]. Left: x-acceleration. Right: z-acceleration

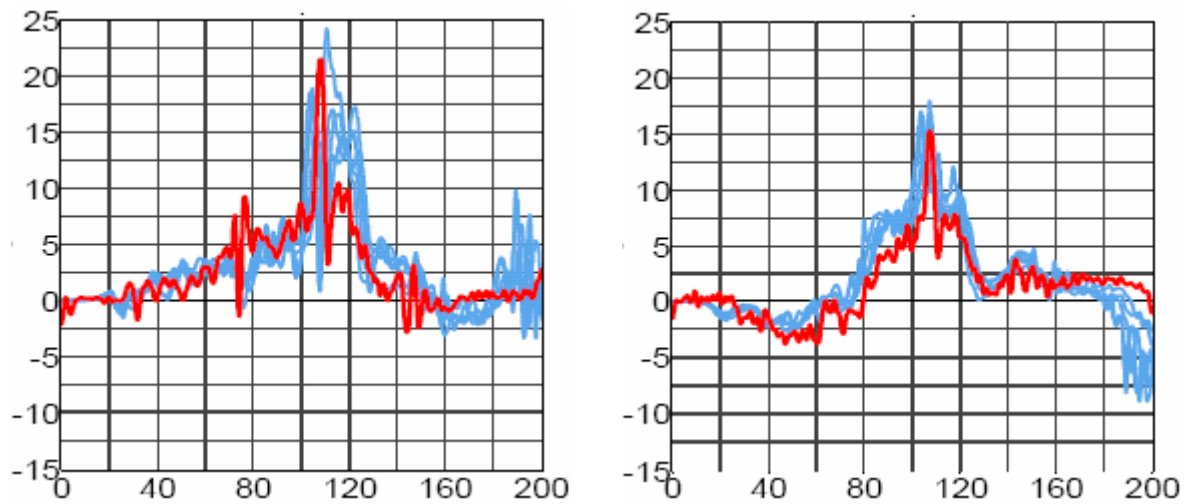


Figure 15: Neck acceleration [g] vs. time [ms] at C4. Left: x-acceleration. Right: z-acceleration.

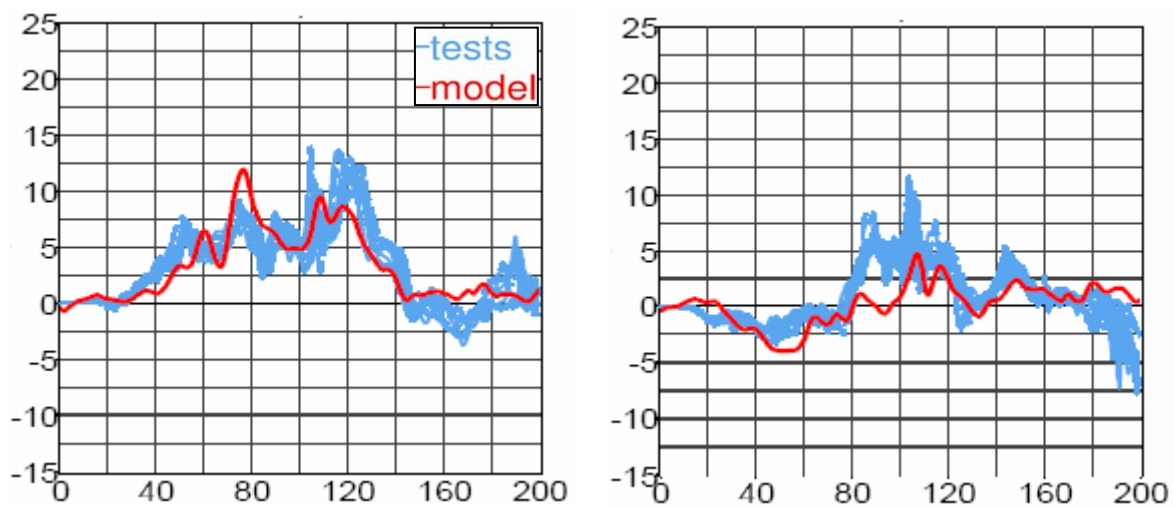


Figure 16: Upper spine acceleration [g] vs. time [ms] at T1. Left: x-acceleration. Right: z-acceleration.

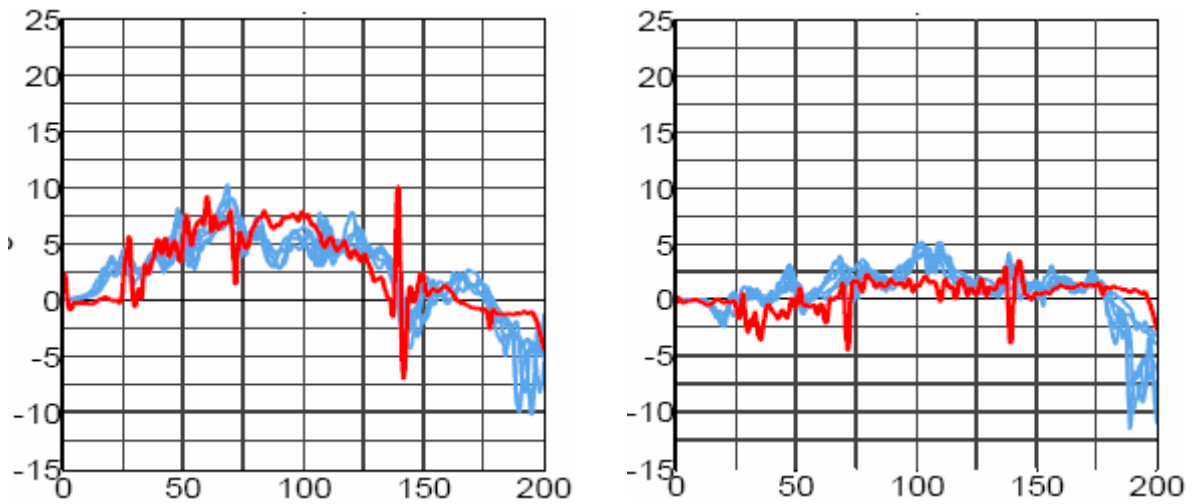


Figure 17: Spine acceleration [g] vs. time [ms] at T8. Left: x-acceleration. Right: z-acceleration.

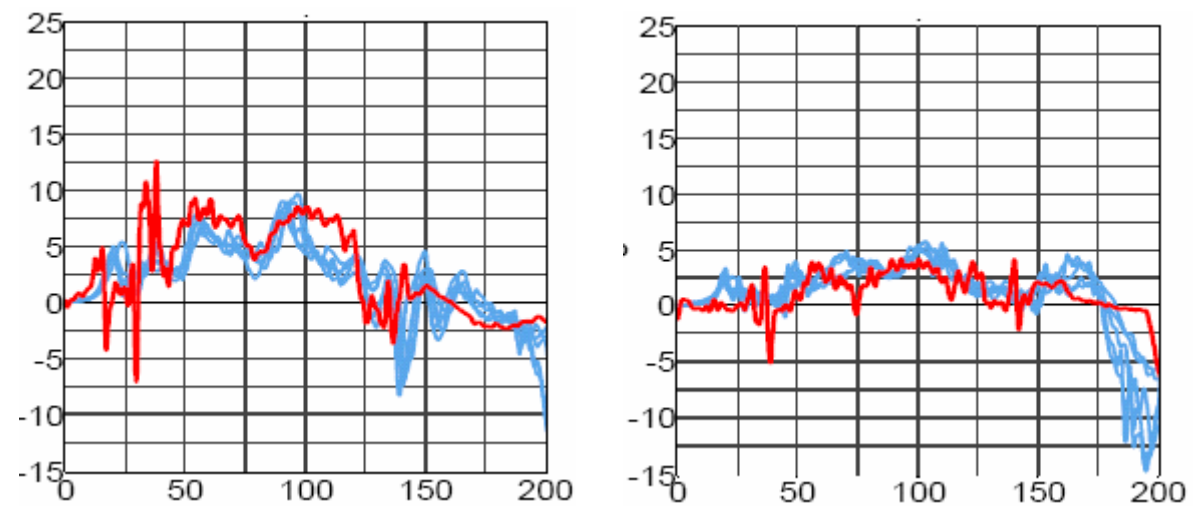


Figure 18: Spine acceleration [g] vs. time [ms] at L1. Left: x-acceleration. Right: z-acceleration

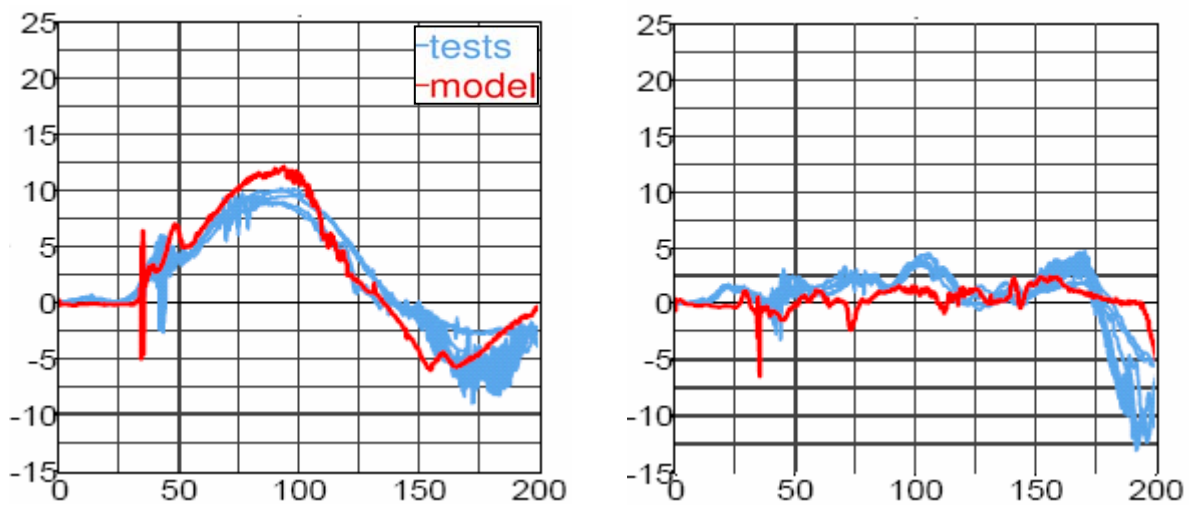


Figure 19: Pelvis acceleration [g] vs. time [ms]. Left: x-acceleration. Right: z-acceleration

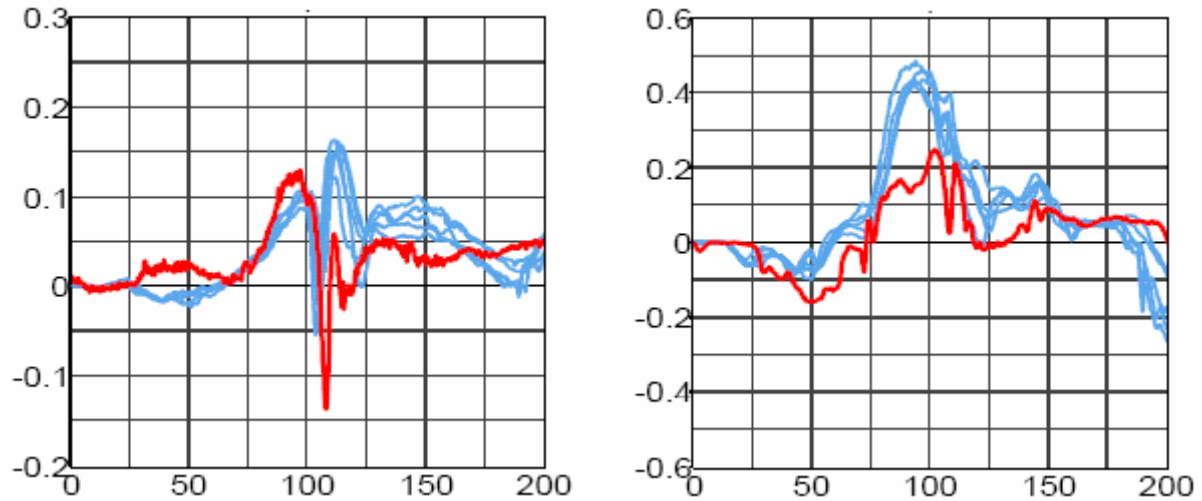


Figure 20: Upper neck force [kN] vs. time [ms]. Left: Force in x. Right: Force in z.

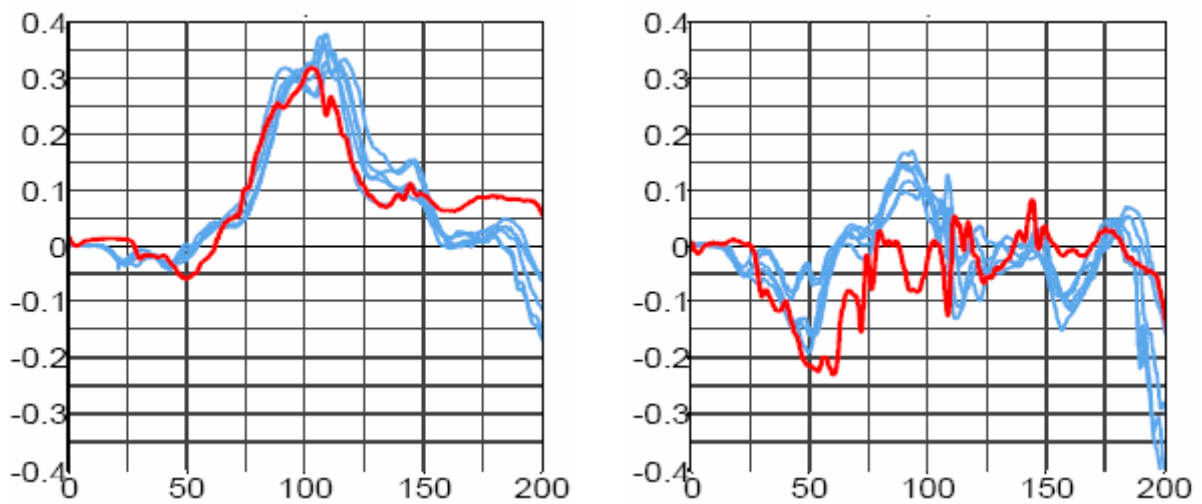


Figure 21: Lower neck force [kN] vs. time [ms]. Left: Force in x. Right: Force in z.

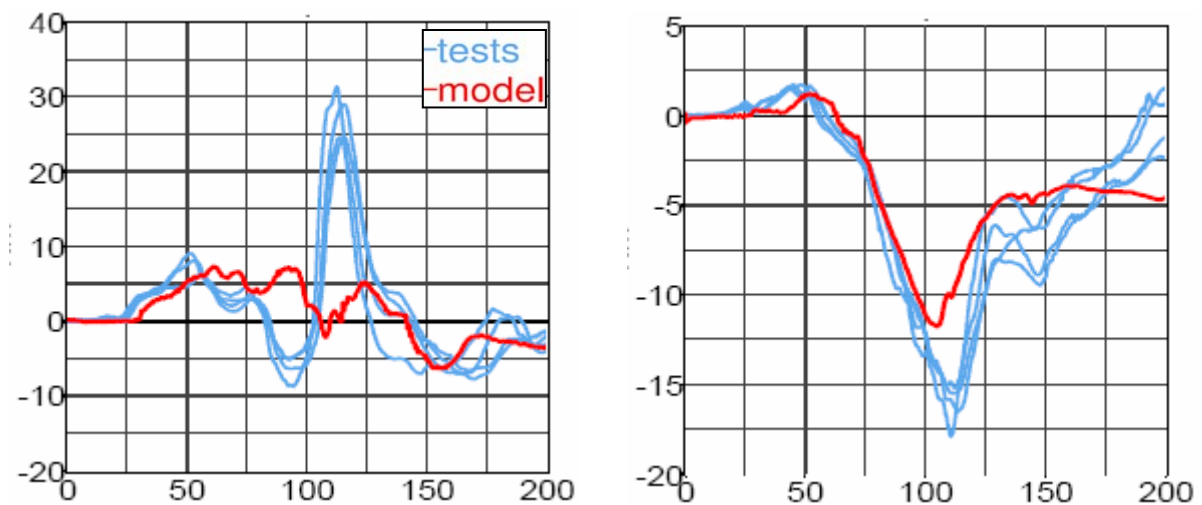


Figure 22: Left: Upper neck moment [Nm] along y axis vs. time [ms]. Right: Lower neck moment [Nm] along y axis vs. time [ms].

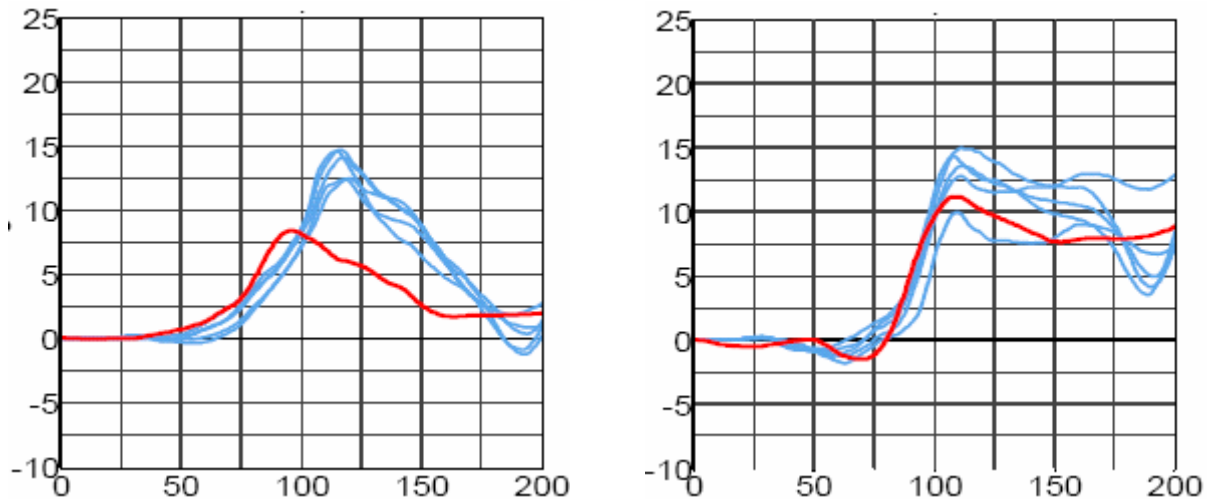


Figure 23: Left: OC neck link rotation [degree] vs. time [ms]. Right: T1 neck link rotation [degree] vs. time [ms].

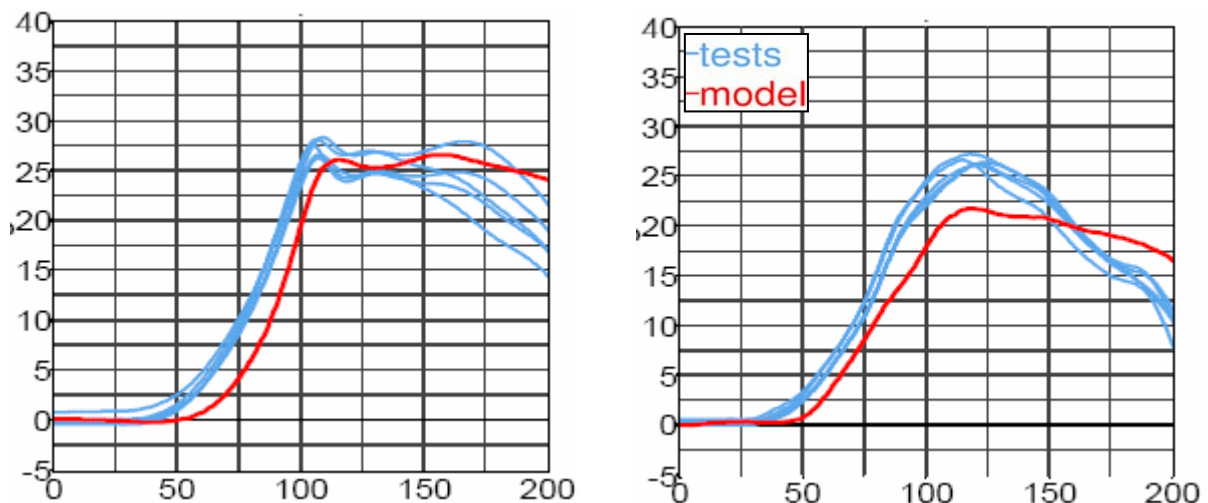


Figure 24: Left: global rotation of head [degree] vs. time [ms]. Right: global rotation of T1 [degree] vs. time [ms].

The quality of the correlation in all tests is comparable to the above presented examples. The accelerations are captured very well. The forces and moments are captured well, but not perfectly. The rotation of the neck link, head and T1 are very difficult to capture. These signals are much more sensitive than the forces and moments.

The reason for the poor correlation in Figure 22 can be explained by the curves in Figure 23 on the left hand side. The neck link rotation is too small which results in different moment arms on the upper neck load cell. Receiving a better performance in the forces and moments is the major current development task.

The current frictional parameters in the model are based on simple assumptions. Currently the frictional values between all interacting parts are measured at the moment. Using the exact frictional value will allow a further model enhancement. Additionally robustness investigations are performed to improve the model.

#### 4 Stochastic Investigations

In the following we focus on the question which parameters have major influences on specific responses and histories (curves). Initially we receive this information by sets of single simulations by varying parameters manually in the input file. Obviously, investigations by running single simulations are limited. Since LS-OPT provides a comfortable tool to investigate the model with stochastically methods, LS-OPT is applied to perform a robustness analysis. In the following selected conclusions of the stochastic analysis are presented.

The full assembled dummy test described in chapter 3.3 with a 5g trapezoidal pulse is used for the stochastic investigations. Some material data, load curves, friction coefficients or damping constants used in the simulation are obtained from tests, therefore the values are subject to some variations. The considered variables for the stochastic analysis are described in Table 1. Unfortunately, the performed tests do not allow determining the variation in terms of statistical quantities of the fuzzy test results. Hence, the scatter of the different parameters is derived from engineering experience and physical assumptions. As an exemption the distributions of "Puls1" and "Puls2" are based on test results. A normal distribution is applied if a target value is available; this target value is defined as the mean value of the distribution. For example, the target value of "Puls1" and "Puls2" is 5g.

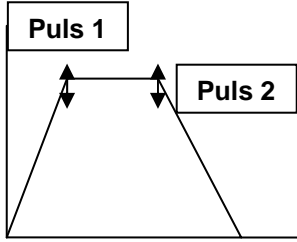
Variable	Description	Distribution		
			lower	upper
mat1010	<b>Material of rubber bumpers yellow.</b> Scale factor of ordinate values for all strain rates.	uniform	0.0004	0.0012
mat1011	<b>Material of rubber bumpers black.</b> Scale factor of ordinate values for all strain rates.	uniform	0.0004	0.0012
mat1025	<b>Material of silicon torso flesh.</b> Scale factor of ordinate values for all strain rates for material.	uniform	0.0006	0.0014
elbow	<b>Rotational stiffness of elbows.</b> Frictional moment limiting value for rotation of elbows.	uniform	3.5	7.0
should	<b>Rotational stiffness of shoulder yokes.</b> Frictional moment limiting value for rotation of shoulder	uniform	12	24
mat1119	<b>Material of pelvis foam.</b> Scale factor of ordinate values for all strain rates.	uniform	0.0007	0.0013
damper	<b>Rotational damper.</b> Damping moment per pitch rate.	uniform	0.2	1.0
con5502	<b>Contact steal seat plate to dummy</b> static and dynamic coefficient of friction	uniform	0.05	0.4
con5514	<b>Contact black rubber mat of seat to back of dummy</b> static and dynamic coefficient of friction	uniform	0.2	0.9
con5501	<b>Contact of break system in the seat</b> static and dynamic coefficient of friction	uniform	0.01	0.3
mat5506	<b>Steel plate of the seat breaking system in the seat</b> scale factor for ordinate values for all strain rates (back frame stiffness)	uniform	0.6	1.0
fric	<b>Steel cable friction in the BioRID neck.</b> Coulomb dynamic friction coefficient.	uniform	0.05	1.3
puls1	<b>Acceleration pulse of sled.</b> The variation of the trapezoid pulse is done by the variation of the vertex of the pulse. This variation is observed in the physical tests. 	normal	mean 5.0	std 0.25
puls2		normal	mean 5.0	std 0.05

Table 1: Variation (distribution) of considered variables for the stochastic analysis

The responses considered in the analysis are listed in Table 2.

response	Description
max_Head_y_angle	maximum angle of head rotation
max_T1_y_angle	maximum angle of T1 rotation
Max_Pelvis_x_accel	maximum pelvis x acceleration
min_lower_Neck_y_moment	minimum peek value of lower neck y moment
max_lower_Neck_x_force	maximum peek value of lower neck x force
NIC	Neck Injury Criteria

Table 2: Responses evaluated for the stochastic investigation

Most figures in this section were created using the software D-SPEX. It is software to explore the design space and to evaluate relationships between variables and responses. Currently, D-SPEX is a stand-alone product from DYNAmore initiated by Audi AG [6], but it will be implemented in LS-OPT. D-SPEX allows the visualization of 2-dimensional curve plots as well as 3-dimensional surface plots. For an n-dimensional problem, where n is the number of design variables and  $n > 2$ , one or two variables can be selected while the other variables values can be varied by a slider. In addition, it is possible to visualize statistical values like mean values and standard deviations, correlation matrix or ANOVA results.

#### 4.1 Monte Carlo Analysis

The idea of a Monte Carlo Analysis is to evaluate the responses at randomly generated sampling points. From the results of these simulations, mean values, standard deviations and other stochastic values can be computed. Here, a Latin Hypercube sampling has been used to generate 200 sampling points. The standard deviation is a measure for the scatter of a random variable around its mean value. The smaller the standard deviation the more values accumulate around the mean value. For the Monte Carlo Analysis of BioRID-II, in total 14 variables and 6 responses are considered, thus each simulation point has 20 dimensions.

##### Example: Normal Distribution (Gauss)

The mean value is denoted by  $\mu$  and the standard deviation by  $\sigma$ .

If a random variable has a normal distribution, the probability, that the value is between  $\mu - \sigma$  and  $\mu + \sigma$  is 0.68 = 68% which is represented by the marked area in Figure 25. The probability that the value is between  $\mu - 2\sigma$  and  $\mu + 2\sigma$  is 0.955 = 95.5%.

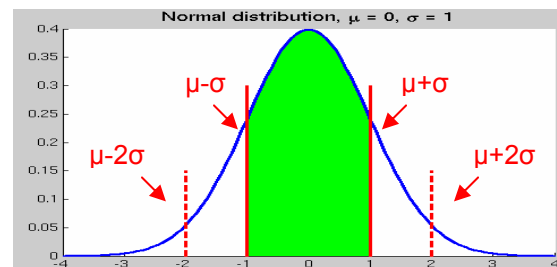


Figure 25: y Density function of probability for normal distribution.

##### 4.1.1 Anthill-Plots

In Figure 26 so called “anthill-plots” of the response values for maximum Head y angle, maximum angle of T1 rotation, maximum lower neck x-force and the minimum of lower neck y-moment versus the variables *mat1010* and *mat1025* are displayed. The solid lines mark the mean values, the dashed lines mark the standard deviations of the variables as well as of the responses.

The torso flesh material (*mat1025*) has a distinctive influence on the maximum T1 and Head rotation. If the stiffness of the material does increase, the maximum rotation of T1 is decreasing and the maximum rotation of the head is increasing. The dependency of the torso flesh material with respect to the maximum T1 and Head rotations is clearly seen. The stiffness of the torso flesh is varied by about  $\pm 40\%$ , the resulting variation of the maximum T1 rotation is about  $\pm 10\%$ .

As a general remark, the interpretation of anthill-plots should be performed carefully in case there is more than one significant variable present. The analysis of trends and dependencies might be wrong and misleading due to the multi-dimensionality of the problem.

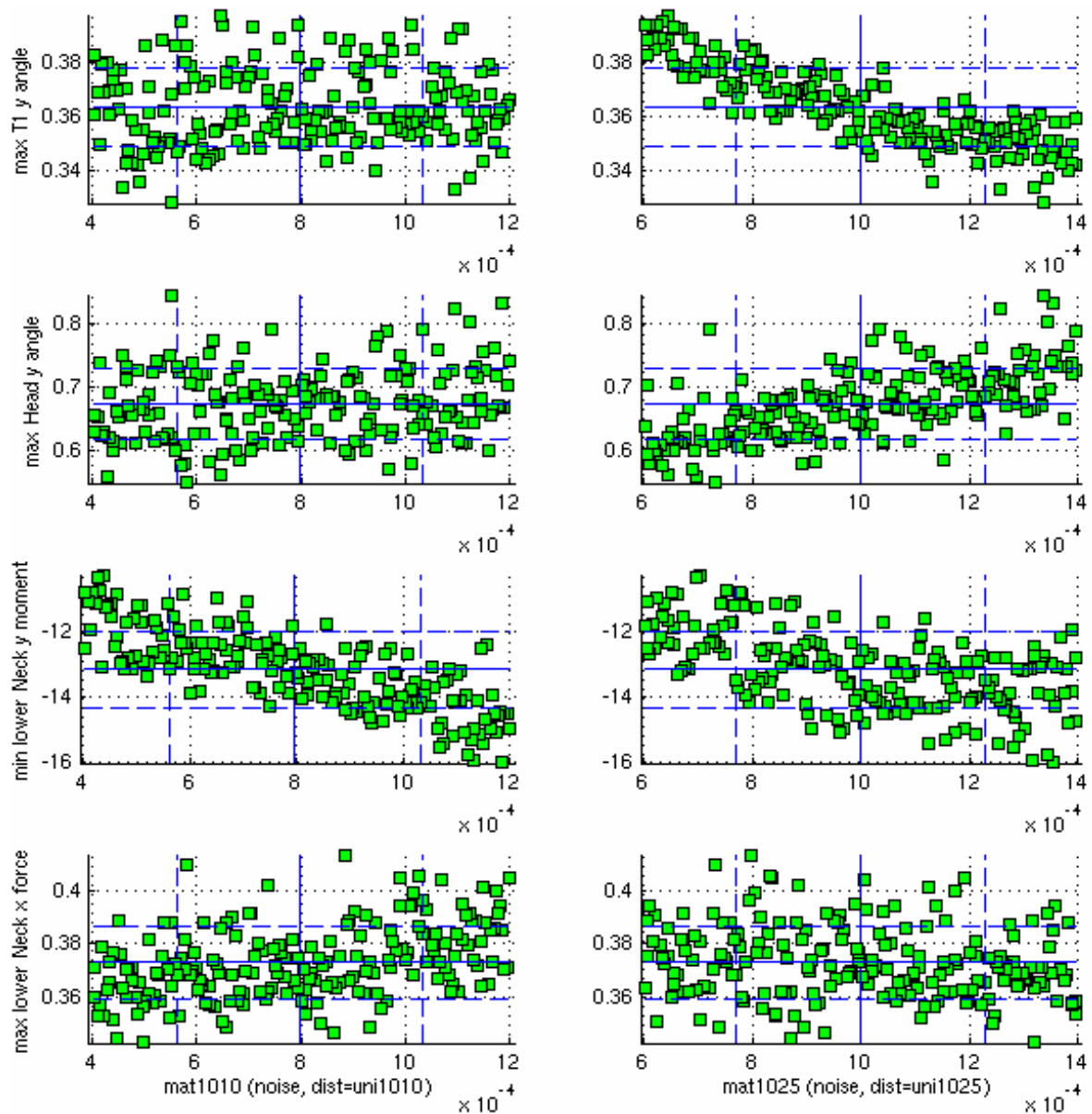


Figure 26: Anthill plot: max\_Head\_y\_angle, max\_T1\_y\_angle, min\_lower\_Neck\_y\_moment and max\_lower\_Neck\_x\_force over mat1010 and mat1025 respectively. Solid line: mean value, dashed line: standard deviation

#### 4.1.2 Correlation Analysis

The matrix in

Figure 27 shows the coefficients of correlation for all responses with respect to all input variables. If the value of the correlation coefficient is close to one or minus one, the field is marked red and the linear dependency of the response on the variable is significant, if the value is close to zero, the field is marked green and there is no significant relationship of the response with respect to the specific variable. Negative sign means that an increase of the input variable leads to a decrease of the output variable (negative correlation).

As already supposed from the anthill plots, variation of variable *mat1025* has the highest influence on the values of the responses *max\_T1\_y\_angle* and *max\_Head\_y\_angle*. Also the variable *Puls1* is significant with respect to the T1 and Head rotations, but its lower compared to the significance of the torso flesh (*mat1025*). This means, the scatter of *max\_T1\_y\_angle* and *max\_Head\_y\_angle* in Figure 24 might result from the variation of the pulse in the physical tests.

A further interesting dependence is the peak value of lower neck y moment. It depends much more on the stiffness of the yellow rubber bumpers (*mat1010*) than the black rubber bumpers (*mat1011*).



Figure 27: Correlation matrix displays significance of input parameters with respect to output values

4.1.3 Stochastic of History Plots

In D-SPEX it is possible to display specific curves of all Monte Carlo simulations in one plot. In addition, the value of an input variable can be visualized by coloring of the curves. So, the user can observe trends of the varying curves due to the variation of the selected variable.

Because of the high significance of the torso flesh material (*mat1025*) in the following some selected history (curve) plots are displayed with respect to the variation of *mat1025*.

The different colors show the value of the variable *mat1025* (torso flesh stiffness) for a specific simulation, but the scatter of the history plots results from the variation of all variables. This is again a problem of the multi-dimensionality similar to the interpretation of anthill plots.

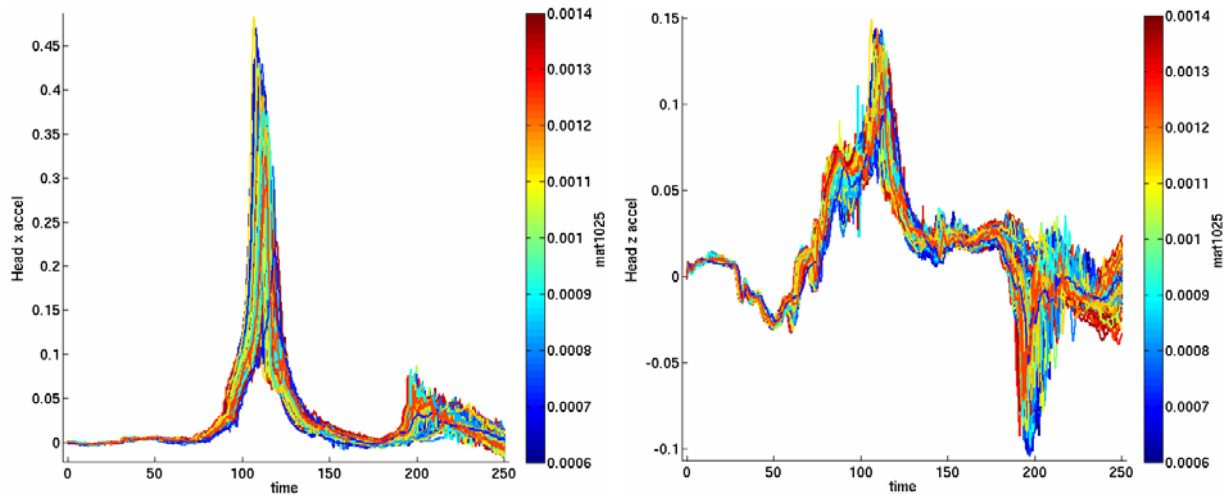


Figure 28: Head acceleration [mm/ms<sup>2</sup>] vs. time [ms]. Left: x-acceleration. Right: z-acceleration.

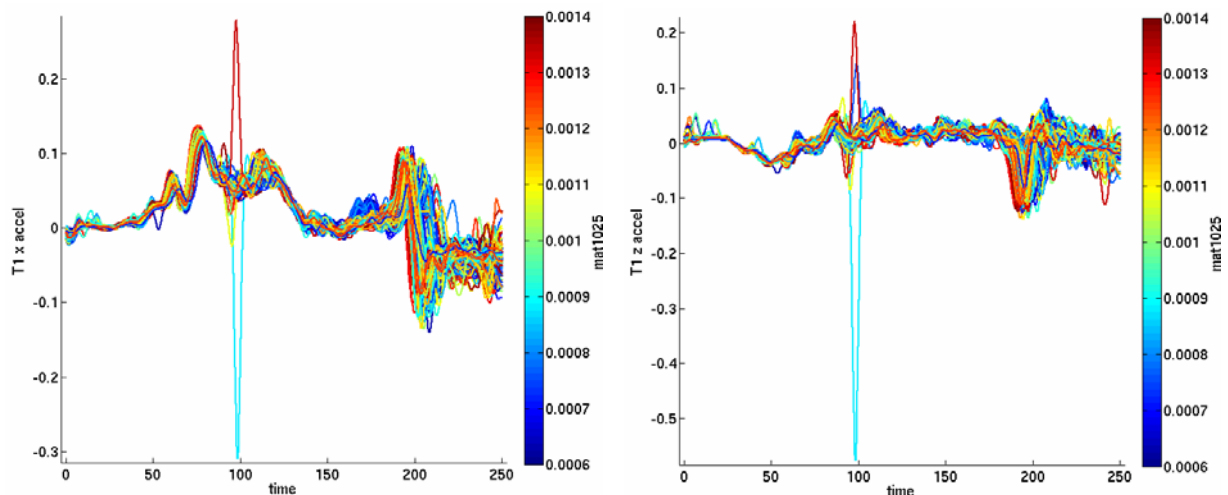


Figure 29: T1 acceleration [mm/ms<sup>2</sup>] vs. time [ms]. Left: x-acceleration. Right: z-acceleration.

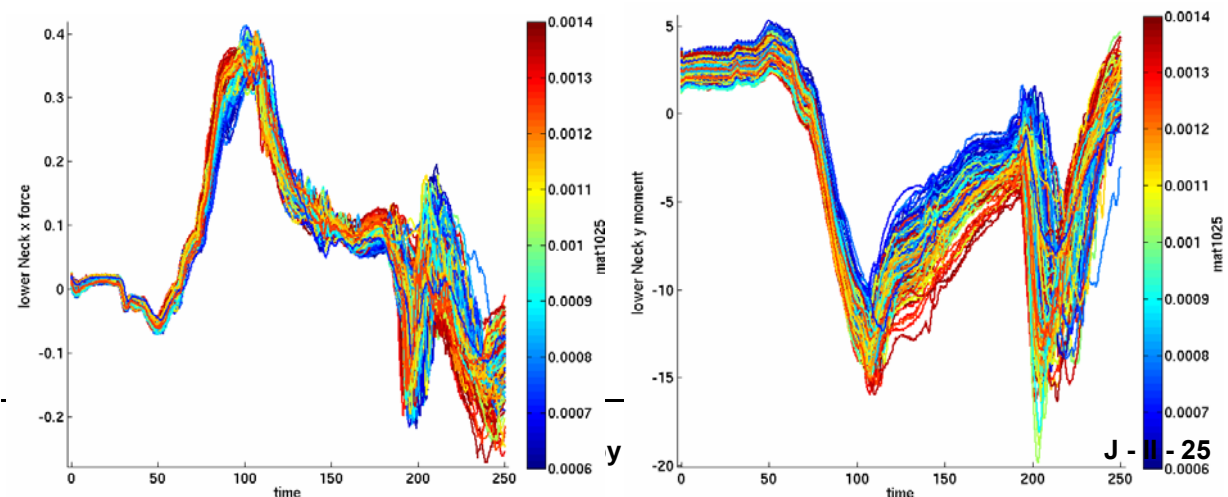


Figure 30: Left: lower Neck x force [kN] vs. time [ms]. Right lower Neck y moment [kNmm] vs. time [ms].

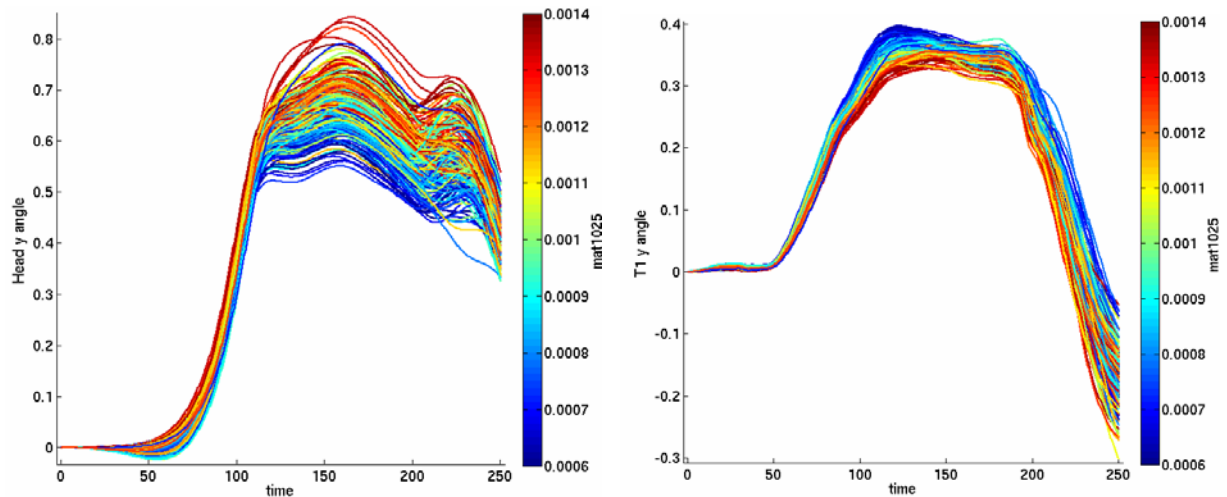


Figure 31: Left: Head global rotation [radian] vs. time [ms]. Right: T1 global rotation [radian] vs. time [ms].

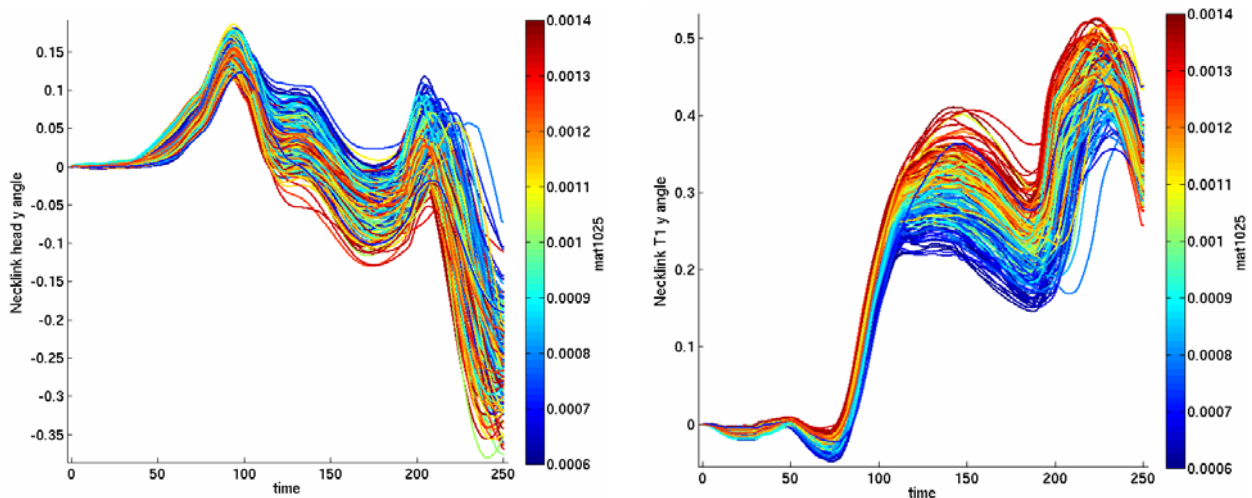


Figure 32: Left: Neck link rotation head vs. time [ms]. Right: neck link rotation T1 angle [radian] vs. time [ms].

In the time history plots it is easy to see, that the scatter in the accelerations is less than in the forces, moments and rotations. This is the reason why the accelerations are mostly easier to predict than some other signals like forces and moments. This observation has also carried out in [4].

A further interesting observation we can see is in Figure 29. In some special situations the acceleration of T1 shows very high peak values. These values are very difficult to handle if we try to extract injury criteria link the NIC from this signals. This peak values in the time histories destroy the scalar values of the injury criteria.

Also notable is, that no observed signal in the history plots is changing its shape. The course of the curves is quite similar.

#### 4.1.4 DYNASTats Evaluation

Using DYNASTats in LS-OPT, statistical values can be fringed on the FE-model. DYNASTats computes the statistical values by extracting physical quantities of each node or element from the d3plot files of all Monte Carlo simulations. The statistical evaluation of those physical quantities can be fringed on the FE-model and displayed by using LS-PrePost. As physical quantities almost all available node and element information of the d3plot database can be applied, i.e. node displacement, velocity or acceleration as well as element quantities such as plastic strain, element thickness, etc.

In Figure 33, the standard deviation of the x-displacements is fringed on the FE model. We observe a very high standard deviation at the hand of the dummy, because its motion is not constrained. At the head, the variation is also quite large because of the large variation of the head rotations. This kind of graphical representation allows the user to detect parts of the model where the scatter of x-displacement is high.

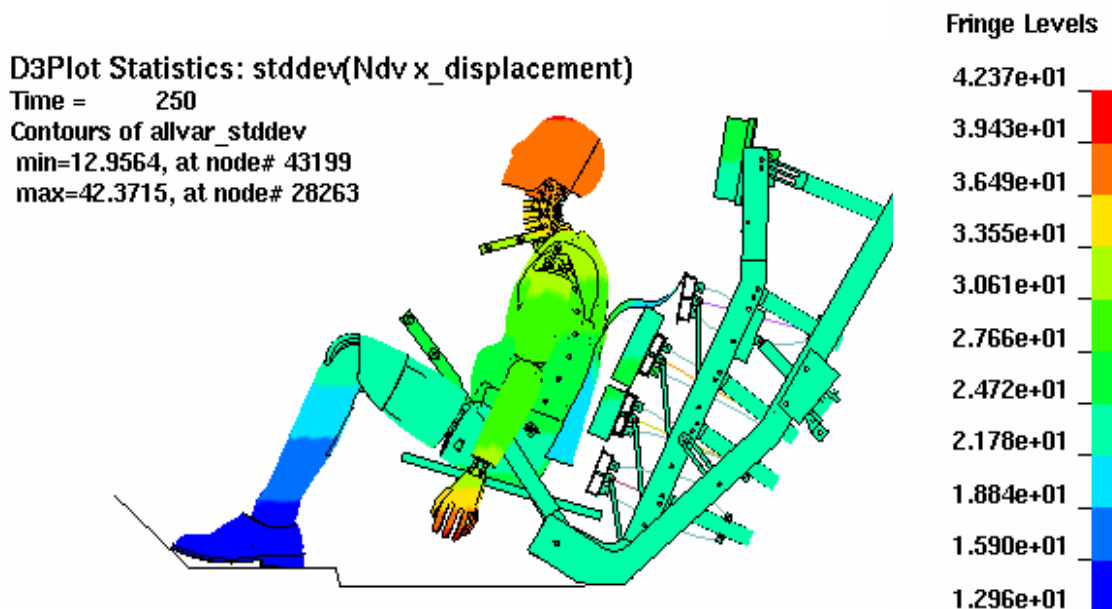


Figure 33: Standard deviation of x-displacement in millimeter resulting from 200 simulations fringed on the FE model

## 5 Conclusions

The current release of the BioRID-II model for LS-DYNA is based on material, component and fully assembled dummy sled tests. The model shows already a good correlation with the extended test data base. By the use of the new material model of the rubber bumpers, the oscillations of the accelerations have decreased significantly. Due to the new material model for the rubber bumpers the next release will require LS-DYNA 971. For selected platforms it is possible to supply an extended LS-DYNA 970 version that includes the required features.

Important knowledge during validation is generated robustness techniques. The paper presents a Monte Carlo analysis of one selected BioRID-II sled test load case. The analysis shows that forces, moments and rotations show higher sensitivities than accelerations. This is in accordance with observations in [4] that signals like accelerations are easier to predict than others such as forces and moments. In addition, an important result of the performed stochastic analysis is the high influence of the yellow rubber bumpers on the lower neck moment.

A more advanced methodology for stochastic investigations is a Meta-Model-based Monte Carlo approach, which is also provided by LS-OPT [7, 8]. Using this methodology is more cost effective, this means fewer simulations are required. Furthermore, using Meta-Models allows visualization of n-dimensional relationships by a continuous 3-dimensional surface. Other variables (if  $n > 2$ ) can be varied by sliders. Doing this interactively helps understanding the model behavior significantly. Performing a Meta-Model based Monte Carlo Analysis for the BioRID-II sled test load case is planned in near future.

The presented methods will be used frequently during development of finite element models from DYNAmore.

## 6 References

- [1] Whiplash (2004), Aspen Opinion, Aspen Re, UK.
- [2] FAT LS-DYNA BioRID-II User's Manual (2006), Version 1.5, DYNAmore GmbH, Stuttgart, Germany.
- [3] P. SCHUSTER, S. STAHLSCHMIDT, U. FRANZ A. RIESER, H. KASSEGGGER, „Entwicklung des Dummymodells BioRID 2“, 4<sup>th</sup> LS-DYNA Forum 2005, Bamberg, Germany.
- [4] Stahlschmidt S., “BioRID-II Dummy Model Development – Influence of Parameters in Validation and consumer Tests”, 9th International LS-DYNA Users Conference Detroit USA, 2006
- [5] BioRID-IIc Rear Impact Crash Test Dummy, James R. Kelly, Robert A. Denton, Inc.
- [6] Thiele M., Optimization of an Adaptive Restraint System Using LS-OPT and Visual Exploration of the Design Space Using D-SPEX, 9th International LS-DYNA Users Conference Detroit USA, 2006
- [7] Stander, N., Roux, W.J., Eggleston, T. and Craig, K.J. LS-OPT Version 3.1 User's Manual, Livermore Software Technology Corporation, March 2006
- [8] Roux, W.J., Stander, N., Günther, F and Müllerschön, H. Stochastic analysis of highly nonlinear structures, *International Journal for Numerical Methods in Engineering*, Vol. 65:1221-1242, 2006.